INVESTIGATING CHANGES IN FAÇADES' ENERGY BALANCE ACCORDING TO COATING OPTICAL PROPERTIES

Maxime Doya[1], Emmanuel Bozonnet[1], and Francis Allard[1]
[1]LEPTIAB, University of La Rochelle, France
mdoya@univ-lr.fr tel: + (33) 5 46458310

ABSTRACT

Cooling energy refurbishment of buildings can be achieved by coating the outdoor walls with paints that have high solar reflectance (0.3-2.5µm) and high thermal emittance (4-80µm). In this presentation, the thermal performance of some paints is studied through an outdoor experiment. In a second part, the inwards conductive flux for a non-insulated wall is modelled with a premise energy budget's module. Lastly, we introduce the construction of a 1/10th reduced scale model of 4 street canyon set to allow the validation of a model coupling mass and thermal transfers between buildings and urban microclimate. Boundary conditions and energy balance are discussed through installed sensors.

INTRODUCTION

Rapid urbanization of the previous 100 years brought along unexpected higher thermal loads in town and particularly in the dense built environment. The resulting phenomenon, called urban heat island (UHI), can be identified by a much higher air temperature in urban areas than the so-called city-characteristic data measured in open-space climatic stations (Pigeon et al. 2008). This UHI is a real concern for health (heat waves and increased air pollution) as for heating or cooling energy demand in the building sector which contributes to the phenomenon increase (Bozonnet et al. 2007). Moreover as growing rates are maintained by the purchasing trend of air-conditioning systems and the population densification, relevant researches have been undertaken to improve the urban environment by integrating passive cooling, solar gains and daylighting. Buildings and microclimatic interactions' aspects of urban planning should be compiled in reliable tools to be use by urban planners (Sailor et al. 2007).

To counterbalance the effects of temperature increase, one of the most efficient techniques proves to be the large scale use of surface coatings presenting a high solar reflectivity and a high thermal emissivity on the urban environment (Akbari et al. 1996). High albedo reduces the amount of solar radiation absorbed through building envelopes and urban structures and thus keeps their surface cooler. A high thermal emissivity allows superior release rates of the energy that have been stored in the inertial mass. These "cool" paints are defined by manufacturers as white and soft tones but for aesthetics' sake, dark and colored tones' paint have been developed (Levinson et al. 2007), (Synnefa et al. 2007). This article gives the results of an experimental platform designed to evaluate surface temperature decrease from different urban coatings. Observations and correlations have been established between the temperatures profile and the other climatic phenomena recorded in order to validate an external surface's energy budget. Secondly, the equation of the surface energy budget is coupled with an air-conditioned indoor space through a conductive response factor method. This part allows the assessment of the indoor consumption evolution implied by the surface temperature differences previously monitored. Thus in the last part, the developments undertaken to measure the energy budget of a reduced scale model of street canyon are discussed.

REVIEW OF KNOWN COOL PAINTS POTENTIAL

Simulated indirect savings at city scale

In some countries, regulations have been implemented in building and energy codes to promote the use of roof coating exhibiting high reflective optical properties (Title 24 California, (Akbari et al. 1996), UE Cool Roof Council[1]). The incentives stipulate the possibility to reduce the roof insulation according to the achieved roof reflectance. This support is the result of intensive simulations and experimental campaigns. At first, meso-scale model have been used to estimate the effects of city-wide changes in surface reflectivity over the regional temperature. Taha (Taha 1997) showed that in mid-latitude warm climate (Los Angeles, south coast basin, CA), increasing the average surface-albedo from 0.25 to 0.4 could bring an average decrease of summer air temperatures of 2 to 4°C. Akbari (Akbari et al. 2003), Rosenfeld (Rosenfeld et al. 1998) also worked over those simulations, their results being reported in a mitigation impact screening tool (MIST). The surface temperature reduction directly mitigates the sensible heat flux convected away of

---

[1] http://coolroofs-eu-crc.eu

the city surfaces, which can be assimilated to a multiple fins heat exchanger, by the surrounding air flow. An indirect gain comes from the incoming outdoor air for cooling machines is lower, thus requiring less power to blow indoor air to the desired set point. Nevertheless, such strategies are long to implement, so far the energy savings have been mainly monitored on isolated buildings.

Direct savings from cool roof experiments

Benefits from cool roofs have been reviewed many times for single story buildings with extended roof surface such as supermarket (Parker et al. 2002), (Akbari et al. 2005), daily peak energy savings ranging from 3 to 52%. The effects of roof solar reflectance on the building heat gain have been mainly explored in hot climates, located under Latitude 23.5° (Suehrcke et al. 2008). The air-conditioning savings or thermal comfort improvements are evident in those places that do not require heating. In floating conditions, maximum daily temperatures of indoor air are only 0.8°C higher than outdoor air for a roof painted having 0.8 solar reflectance. The observations on experimental sites prove that savings are inversely correlated with the amount of ceiling insulation and the location of AC duct systems. Simulations have been carried out for different locations on TRNSYS thermal simulation software (Synnefa et al. 2007), modeling an isotropic, flat roofed, low-rise building, the results tends to prove that the heating penalty are less important than the cooling load reduction for countries located between 19.19° (Mexico, Mexico) and 43.4° (Nice, France). Nevertheless, for a roof reflectance of 0.65 and a roof thermal resistance of 0.84W/m².K, the changes in cooling and heating loads for France's location seem fairly equal as seen in Figure 1 that allows us to wonder if the change is worth being done.
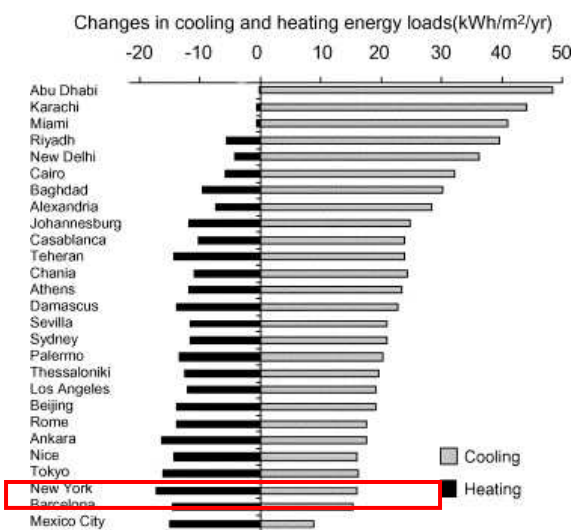
Figure 1: Climate effects on cooling and heating load changes for a change in roof solar reflectance of 0.65, source: Synnefa et al 2007

Considering the case of isolated buildings, the air conditioning demand is mainly influenced by heat loads from the roof. Very little studies have been led on the impact of façade optical design on the building thermal loads. In Hong Kong, test cells have been installed to study the effect of color on indoor temperatures in hot humid climates (Cheng et al. 2005). They reported that for lightweight construction, the maximum air temperature inside the black cell was higher by about 12°C than that of the white cell. Additionally the air temperature inside the white cell was only 2-3°C higher than outside. Their results also show that the influence of color was dependant to the solar radiation; the darker the color the more sensitive to solar radiation.

Interchanges effect

More specifically in urban centers, confinement of surfaces leads to multiple reflections of thermal radiative energy. Most of the radiation first reflected is re-intercepted and partially absorbed by other urban surfaces. Surface-albedo modifications bring up evolutions of energy budget at the interface between building envelope and outdoor environment. Thus changing conductive heat transfer towards the premises and temperatures of the air bulk between the pavement and the urban canopy (Doya et al. 2007). Our research is based on the consequence of the configuration of surface optical coefficient in an urban street canyon (USC), where the radiative interactions between buildings are quite important. This interaction is scarcely taken into account in building energy simulation excepted by solar masks computation. Focus on the USC has been chosen because this basic urban shape has been extensively studied on airflow purposes; consequently, several airflow algorithms applied to the inner canyon depending on prevailing winds above the canopy are available.

SURFACE ENERGY BUDGET

An experimental platform has been set up in order to investigate the exterior energy budget of horizontal painted surfaces exposed to local climatic variations in La Rochelle, France. Sensibility patterns of the thermal exchanges occurring at the surface and hourly variations of the boundary conditions has to be evaluated, thus allowing to assess the accuracy of radiative and convective coefficients used in our simplified coupled models. We needed to measure accurate surface temperature, so nine discs have been specially designed with 2 thin Kapton© leaves, this insulation material covers an integrated type K thermocouple, themselves coated with 0.25µm copper film. Those discs have been painted with the chosen products, fixed on a thick insulated rack with double-sided tape in order to neglect the downward conductive heat transfer on the rear face, and the edges have been sealed with resin, thus cutting off the convective draught under the plates. Using

paints' optical coefficients from a spectrometric pre-study (Table 1), the measurements of far infrared irradiation from the sky, of incident solar radiation, of air and surface temperature profiles of 9 thin paint coated copper plates insulated on the downwards face, we can close the surface energy balance equation and deduce the convection flow.

Table 1: Spectral reflectivity of presented samples

COLOR AND TYPE	VIS 0,38-0.78μm	NIR 0.78-2.5μm	Global SR 0.28-2.5μm
Soprastar Flam®	0.762	0.769	0.744
Slate-Black shingle	0.066	0.062	0.064
Anthracite Cool paint	0.102	0.413	0.235
Black Std paint	0.081	0.045	0.050
Brown Cool paint	0.123	0.401	0.241
Brown Std paint	0.132	0.146	0.134
Green Cool paint	0.127	0.426	0.254
Green Std paint	0.06	0.107	0.08
Dark Blue Cool paint	0.223	0.383	0.292
Light Blue Std paint	0.205	0.379	0.277
White Std paint	0.900	0.879	0.865

The table values represent the visible (VIS) spectra reflectivity and near infrared (NIR) spectra and thus the global solar reflectivity over the currently considered solar spectra. The cool paints studied, have been traditionally prepared in the University of Athens, and they are not optimized products. On the second hand thermal emissivities have been also measured with an Emissometer AD model, but the shingle samples exhibited a subsequent thermal capacitance which induced a substantial error, because of this, we have reevaluated the coefficient by data observation. On top of that, local wind speed and direction were recorded in order to compare and assess convective empiric equations developed in extended literature.

Traditional and cool paint samples

In Figure 2, daily surface temperature recordings of the nine colour samples described beforehand are displayed as well as the incident atmospheric long-wave radiation and solar short-wave radiation. At the maximum peak temperature (15h00), the white paint is 18°C cooler than the black that reaches 49°C, and the blue cool and standard coatings are the second cooler surfaces with 6.5°C under the black one.

Figure 3 allows estimating the thermal emissivity values of our samples relatively to a control sample; it represents the nocturnal occurrence of temperature difference between a control sample and the 8 others.
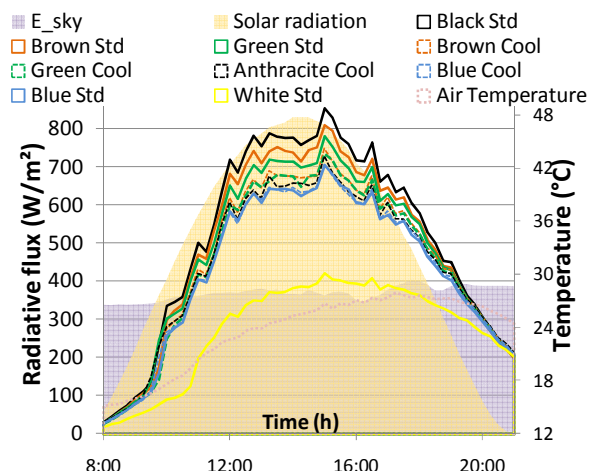
Figure 2: Evolution of surface temperature according to their colour and solar and longwave radiative fluxes on the 27th of August 2008
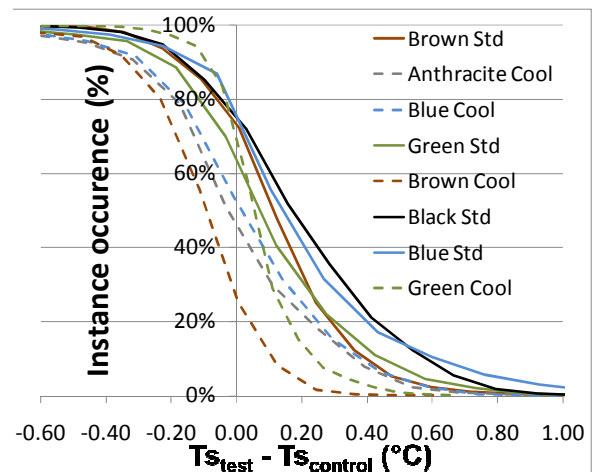
Figure 3: Occurrence of nocturnal temperature difference between the 8 tested colours and the control white sample in cumulative frequencies from the 10th of Dec to 10th of Feb 2009.

In that case, compared to white surface temperature, the night temperature difference between all 9 samples evolves between -1.9 and 1.8°C. By observation of the respective area covered by the different ΔT and by arbitrarily deciding the white emissivity measurement as right, long-wave emissivity coefficients have been attributed to each sample. The Figure 4 represents the diurnal occurrence according to the same process. Here, the temperature trends respect fairly well the magnitude of solar reflectances measured. The occurrences where colored sample temperatures are lower than the white sample are due to rain or frost episode. We notice that the dark blue cool is lower than light blue standard temperature; that is mainly due to the soiling and weathering effect on the paints' surface after one year of exposure. The temperature difference between the white and black samples are under 3°C during 40% of the time, 6°C for 10% and can reach 11°C on particularly sunny winter days.
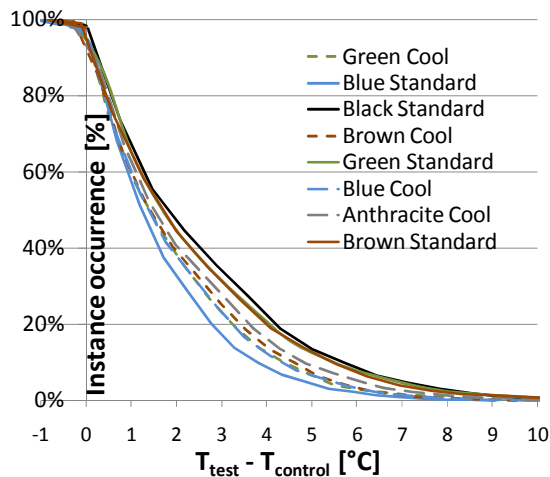
Figure 4: Occurrence of diurnal temperature difference between the 8 tested colours and the control white sample in cumulative frequencies from the 10th of Dec to 10th of Feb 2009.

Roof waterproof Shingle

In parallel with the paints' experimental bench, we set the same experiment on roof shingle 20x30cm samples. The temperatures and the conductive fluxes were measured under the 2 to 4mm thick samples. The Figure 5 illustrates the evolution of a sample duo's surface temperature, 3 high absorbance black shingles and 3 high reflectance Soprastar Flam® samples during 3 winter days, in parallel with air temperature, sky long-wave radiative flux and solar shortwave radiative flux.
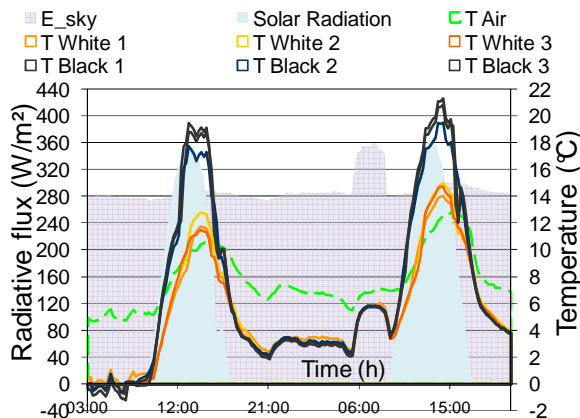
Figure 5: Air, surface temperatures and incident radiative fluxes recorded from 22 to 25th of January

During the winter period in La Rochelle, air temperature evolved between 4 and 13°C, and in spite of a small solar radiative flux (<400W/m²) the maximum temperature difference between the high reflective coating and the absorptive one was 11°C during the day. An average difference temperature has been calculated at 1.5°C, and it has been observed that the black shingle samples are cooler during the night, this feature is probably due to a higher thermal emissivity. The Figure 6 shows the temperature difference between the two same samples as cumulative relative frequency from the

10th of December to the 10th of February. Diurnal behavior of the sample surface difference is clear, 96% of the period, the white sample temperature is lower than the black shingle one. Fifty percents of the time the difference spread between 0 and 2°C but the maximum can reach 14°C. Nocturnal behavior is not as neat to determine, during 86% of the night period, the black shingle is cooler. This feature is due to its higher emissivity; nevertheless 50% of that difference is spread between 0 and 0.1°C, meanwhile the difference can fluctuate between -1.8 and 2.1°C.
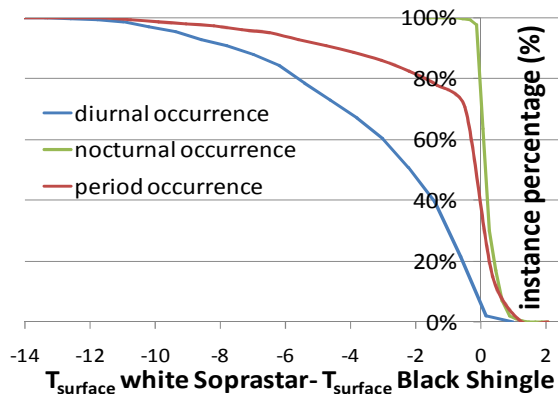
Figure 6: Temperature difference of a white smooth roof coating and a black shingle in cumulative frequency over 2 months.

The sample emissivities differ from one or two hundredths and the convective surface coefficient plays an important role in such small temperature difference. We supposed the convective heat transfer coefficient equal for all samples, but it also depends on the sample roughness and the wind angle on the sample platform. The convective heat transfer coefficients have been evaluated during summer nights without condensation episode and have a good agreement with empirical Turbulent Reynolds equations.

WALL ENERGY BUDGET

In fact, the sensitivity to heat transfer modes of a building wall is strongly dependent of the optical properties of its surfaces, of its thermal resistance and its thermal capacitance. In order to assess the real behaviour of a wall, in this part a simple indirect calculation method is developed to calculate the transient conductive heat transfer coupled with the surface energy budget.

Response factors for conductive heat transfer

A 1D finite-difference method is used at first to match multi-layer walls response to unit temperature step input on both surfaces. Then the heat response obtained is sampled according to the required frequency (hourly). In our model, the heat conductive flux must remain under a simplified indirect form, radiative and convective fluxes expressions must be corraled to the surface node temperatures (indoor surface temperature T_{SI} and external surface

temperature, T_{SE}) consequently they must not be included in a surface exchange coefficient, and the heat conductive transfer is considered between the two surface temperatures. At any time n [hour], the heat conduction through a wall to the interface between the indoor wall surface and the indoor air consecutive to input temperature steps on both wall surfaces can be calculated by the general response factors in the following equation:

$$\Phi_{cond}^{int}(n) = \sum_{j=0}^{N} Y_j . T_{SE,(n-j)} - \sum_{j=0}^{N} X_j . T_{SI,(n-j)}$$

Thus, the heat conduction through a wall to the interface between the outdoor wall surface and the outdoor environment consecutive to input temperature steps on both wall surfaces can be represented by:

$$\Phi_{cond}^{ext}(n) = \sum_{j=0}^{N} Y_j . T_{SI,(n-j)} - \sum_{j=0}^{N} Z_j . T_{SE,(n-j)}$$

X_j, Y_j, Z_j are the periodic response factors of conductive heat transfer specifically sampled according to the selected simulation time basis. One can truncate the response factors' series depending on the wall's thermal properties and the user's required accuracy. The surface temperature depends on the surface heat budget (see *Figure 7*).
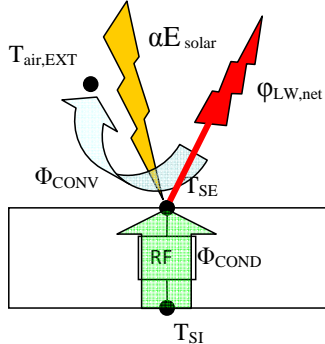
Figure 7: Pattern of energy fluxes at outdoor surface

The surface balance can be written as:

$$\varphi_{conv} + \varphi_{LW,net} - \alpha_{SW} . E_{solar} - \varphi_{cond} = 0$$

Then φ_{cond} is developed in the response factors' fashion:

$$h_{cv}^{local}(T_{SE} - T_{air}^{ext}) + \varphi_{LW,net} - \alpha . E_{solar} \\ = (Y_1 T_{SI} + YTSI - Z_1 T_{SE} \\ - ZTSE)$$

With Y_1 and Z_1, the first response factors for the wall, *ZTSE* and *YTSI* are constant terms depending of the *N*-1 previous indoor and outdoor surface temperature values and the *N*-1 other response factor terms:

$$ZTSE = \sum_{j=2}^{N} Z_j T_{SE,(N-j)}$$

$$YTSI = \sum_{j=2}^{N} Y_j T_{SI,(N-j)}$$

h_{cv} is the local convective heat transfer coefficient at the roof surface. α_{SW} is the solar absorption coefficient and E_{Solar}, is the incident solar radiation to

the considered wall in W/m². φ_{LW} is the net external surface long-wave radiative flux in W/m². X_1, Y_1, Z_1 are the initial response factors of the considered multilayer wall and *YTSE* and *ZTSE* are the sum of superior order response factors at previous instants. At the inner surface, radiative and convective heat transfers have been linearized with a global heat transfer coefficient, h_g and a radiative resultant temperature T_{RS}:

$$h_g . S(T_{SI} - T_{RS}^{in}) = (Y_1 T_{SE} + YTSE - X_1 T_{SI} - XTSI)$$

$$YTSE = \sum_{j=2}^{N} Y_j T_{SE,(N-j)}$$

$$XTSI = \sum_{j=2}^{N} X_j T_{SI,(N-j)}$$

As we consider only the transfer within a wall through this simplified model non-coupled with the premises other heat loads, only inwards and outwards values of the heat transfer at the indoor wall surface are investigated. An indoor set point temperature is arbitrarily set for the summer season and it should match with internal gain effects. The inwards heat transfer is counted positive and the outwards one is negative.

Modelling cooling energy savings and heating losses according to solar reflectivity

In the following graphs, the outdoor air and effective sky temperature have been approximated with a sine function in order to match with a typically hot day in June 2008:

$$T_{amb,av} + T_{amb,amplitude} \times \sin\left(2\pi + \frac{t - period}{24}\right)$$

For the summer period, the average ambient temperature for the day has been set at 26.9°C, the temperature amplitude at 5.1°C and the period at 12.2 hour. According to the same equation, an effective sky temperature has been simulated, with a 0°C average temperature and 5.6°C amplitude. The day has been repeated several times as an input in order to reach the stable thermal conditions. Three solar absorptivities have been considered and the spectral thermal emissivity has been conserved to 0.9. The first absorptivity of 0.95 corresponds to a mat black new paint, 0.75 is its equivalent "cool" derivative and 0.15 is the maximum reflectance that a white commercially available urban product can achieve. Figure 8 showed the indoor and external surface temperatures for the three configurations on a typical hot summer day in La Rochelle. The graph points out a 14°C difference between the indoor surface temperatures of the high and low absorptive cases; and maximum 25°C for the outdoor wall surfaces. Another characteristic of this graph is the peak temperature's time lag, the maximum temperature occurs at 17h00 in the 0.75 and 0.95 cases, meanwhile it approaches 19h00 for the 0.15 one.
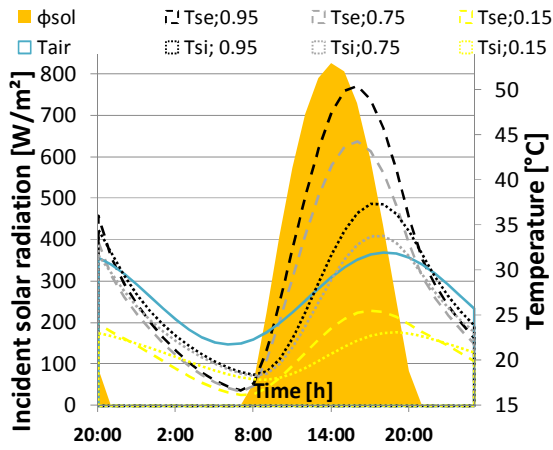
Figure 8: Surface temperatures of a 12cm walled concrete wall according to its solar absorbance during a clear summer day

As for Figure 9, the curves correspond to inwards and outwards conductive fluxes achieved by the different absorptivities for the same day, plus the outside air and sky effective temperature:
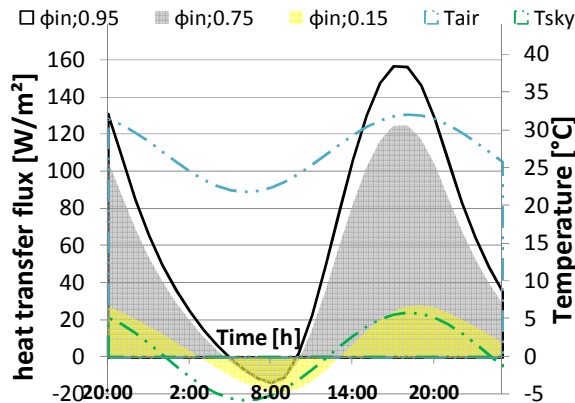
Figure 9 : Conductive heat fluxes of a 12cm walled concrete wall according to its solar absorbance during the same hot summer day

Considering the values of the peak flux, we can see that for the 0.75 configuration, the inwards conductive flux to fight up has been decreased from 20.5% compared to the 0.95 one, and from up to 80% for the 0.15's one. The daily heat transfer rates are summarised in the Table 2.

Table 2 : Heat transfer rates in Summer

ABSORPTIVITY	0.95	0.75	0.15
Average T_{SE} [°C]	31.0	28.5	20.8
Inwards conductive energy [kWh/m².day]	1.51	1.19	0.23
Outwards conductive energy [kWh/m².day]	-0.04	-0.05	-0.12

For the winter period, the average ambient temperature for the day has been set at 8.5°C, the temperature amplitude at 4°C and the period at 10 hours. The sky effective temperature has the same characteristics as for a summer day. The Figure 10 shows the surface temperatures for the wall in winter:
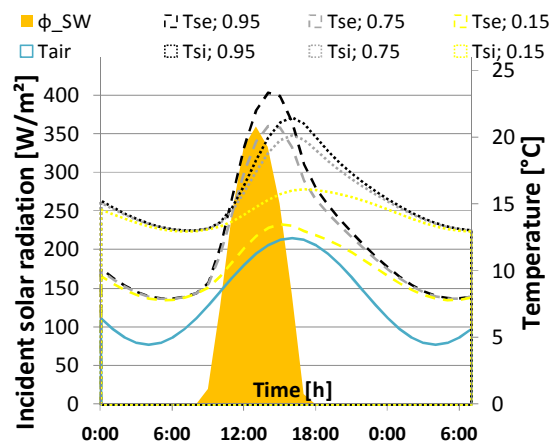
Figure 10: Surface temperatures of a 12cm concrete wall according to its solar absorbance during a clear winter day

During the afternoon peak temperature, the graph reveals only a 5.4°C difference between the indoor surface temperatures of the high and low absorptive cases; and maximum 10°C for the outdoor wall surfaces. Here too, the time lag for the maximum wall surface temperature intervenes 2 hours later for the high albedo configuration. The Figure 11 shows the corresponding inwards and outwards heat transfer at the inner surface:
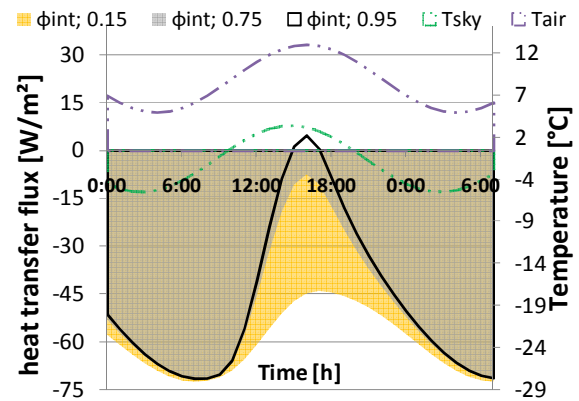
Figure 11: conductive heat fluxes of a 12cm walled concrete wall according to its solar absorbance during the same hot summer day

At the maximum peak, the inner wall of the 0.15 configuration loses 83% more heat than the wall with the 0.75's solar absorptivity. Concerning the 0.95 wall, it receives an hourly heat transfer of 5Wh/m² at 16h00, so relatively to the white configuration, heat transfer losses are 110% lower. Table 3 show the daily heat transfer rates coming in and out of the walls considered.

Table 3 : Heat transfer rates in winter

ABSORPTIVITY	0.95	0.75	0.15
Average T_{SE} [°C]	13.5	12.7	10.5
Inwards conductive energy [kWh/m².day]	0.01	0.0	0.0
Outwards conductive energy [kWh/m².day]	-1.02	-1.11	-1.41

Results and discussions

The climatic inputs chosen for the summer simulations are extreme in La Rochelle. Consequently, the white configuration, usually employed to diminish some cooling energy, does not look attractive. Yet, on those two simulated days, there is 85% reduction of the inwards heat transfer in summer for the high albedo compared to the low one; in the winter case, the daily outwards flux to compensate is only 28% lower in the case of the higher albedo surface. The results for T_{SE} are comparable with the surface temperatures obtained with the experimental bench, with a difference. The optical surface coefficient value has to be chosen in order to balance the annual inwards and outwards heat transfer rates. The simplified model we developed gives a first approximation of the expected thermal performances. Nevertheless, the model has to be completely coupled to have a good approximation considering the local urban environment and the indoor strategies (internal gains, ventilation...). The development of the complete model is going along with an operation of validation thanks to an experimental campaign.

REDUCED SCALE MODEL OF URBAN STREET CANYON

The performances described previously are valuable for unidirectional wall surface exposed to specified radiative fluxes and specified air temperature. In the complete code we have developed, the equations of the premises model are coupled with the microclimate model of a USC. A first study ((Doya et al. 2007) demonstrated the potential of this technique; however, comparisons with experimental data are needed to validate this model. On this purpose, a $1/10^{th}$ reduced scale model of 4 urban street canyons has been configured to study 4 different strategies. In order to match the real urban environment, the reduced scale model needs to comply with dynamical and geometrical similarities.

Requirement of physical similarities

Radiative similarity is fulfilled as long as we are using actual building materials (painted walls and concrete pavement) because the dimensions of a scale model are always superior to the wavelengths in consideration in radiative heat transfer mode (Kanda 2006). The buildings composing each USC have been matched by three rainwater tanks, built with a walled mix of concrete and metal, 7cm thick, they can be considered as equivalent to lightweight construction (Figure 12). Concrete and reinforced concrete are current material of use in building construction; consequently, the thermal conductivity and thermal inertia are matched.

Figure 12: Experimental platform unprepared

Configurations

The 4 urban street canyons at our disposal will be soon configured according to the following pattern:
A control street painted with a standard stone color, a cool street coated with a colored paint with high reflectivity in the near Infrareds, an asymmetric canyon with the 2 kinds of façades, and the last one has similar façades to the control street one but flat green roofs will be set on the top of the rainwater tanks. This last street will allow the comparison of the performance of those two passive cooling strategies.

Measures under consideration

The USC are equipped in order to measure the input data of our numerical code. To precisely close the energy balance on specific unit surface, a pair of thermocouple is fixed under a thin layer of concrete on indoor and outdoor surfaces of the envelope in order to measure local conductive transfers. And on the same point, a heat radiative sensor is associated. The solar radiation onto any point of the scaled urban scene can be accurately defined thanks to the radiosity method knowing the horizontal solar irradiance on the experimental platform as an input. Those settings will allow a good estimate of the local convective heat transfer sensibility and its coefficient (CHTC). The similitude with the turbulent airflow characteristics are not respected so wind speed and direction would not be reliable investigations, hence we measure their value only at a local point one meter above the urban canopy through a wind-vane anemometer. A first calibration period will be done with the 4 USC painted in the same fashion. The monitored data of this period will be used to realize a relative estimate of wind speed near the 4 canyons surfaces thanks to empirical equations liking the CHTC and the wind speed. Surface and air boundary temperatures are measured at some points easily repairable in the numeric zonal model representative of the under canopy bulk. The air temperature thermocouples are set into high reflective metallic tubes in order to get a protection from surrounding radiative transfers. They are mounted on a threaded stick, giving us the choice to adjust the distance of

measurement relative to walls. A rain gauge has been disposed on the site in order to allow a pruning of our data on certain days because we suppose the latent heat exchange term as nil in our model.

CONCLUSION

The surface optical coefficients have been arbitrarily set at extreme values for the simulations. The heat transfer through the wall is positively balanced for the high albedo configuration since it allows a really good passive cooling in summer (85% more than the low albedo configuration) and on the other hand the winter penalties counteract only 28% higher than the black configuration. The differences obtained on the experimental bench and through the simplified model for the surface energy budget seems to match with a good order of approximation. Yet, assessment of the thermal performances of any architectural strategies deserves to be studied along with its local microclimate. Their interaction effects are still not totally indentified; consequently, the development and observation of a reduced scale model of an urban scene is essential in our case.

ACKNOWLEDGEMENT

REFERENCES

Akbari, H., R. Levinson, et al. (2005). "Monitoring the energy-use effects of cool roofs on California commercial buildings." Energy and Buildings **37**(10): 1007-1016.

Akbari, H., A. H. Rosenfeld, et al. (1996). Policies to reduce heat islands: magnitudes of benefits and incentives to achieve them. ACEEE Summer Study on Energy Efficiency in Buildings, Pacific Grove, CA.

Akbari, H., L. Shea Rose, et al. (2003). "Analyzing the land cover of an urban environment using high-resolution orthophotos." Landscape and Urban Planning **63**(1): 1-14.

Bozonnet, E., R. Belarbi, et al. (2007). "Thermal Behaviour of buildings: modelling the impact of urban heat island." Journal of Harbin Institute of Technology **14**(Sup.): 19-22.

Cheng, V., E. Ng, et al. (2005). "Effect of envelope colour and thermal mass on indoor temperatures in hot humid climate." Solar Energy **78**(4): 528-534.

Doya, M., E. Bozonnet, et al. (2007). Theoritical evaluation of energy performance achieved by "cool" paints for dense urban environment. CLIMAMED 2007 Genova, Italy, AICARR

Kanda, M. (2006). "Progress in the scale modeling of urban climate: Review." Theoretical and Applied Climatology **84**(1): 23-33.

Levinson, R., H. Akbari, et al. (2007). "Cooler tile-roofed buildings with near-infrared-reflective non-white coatings." Building and Environment **42**(7): 2591-2605.

Parker, D. S., J. K. Sonne, et al. (2002). Comparative Evaluation of the Impact of Roofing Systems on Residential Cooling Energy Demand in Florida. 2002 ACEEE Summer Study on Energy Efficiency in buildings, Pacific, California.

Pigeon, G., A. Lemonsu, et al. (2008). "De l'observation du microclimat urbain à la modélisation intégrée de la ville." La Météorologie **62**: PP. 39-47.

Rosenfeld, A. H., H. Akbari, et al. (1998). "Cool communities: strategies for heat island mitigation and smog reduction." Energy and Buildings **28**(1): 51-62.

Sailor, D. J. and N. Dietsch (2007). "The urban heat island Mitigation Impact Screening Tool (MIST)." Environmental Modelling & Software **22**(10): 1529-1541.

Suehrcke, H., E. L. Peterson, et al. (2008). "Effect of roof solar reflectance on the building heat gain in a hot climate." Energy and Buildings **40**(12): 2224-2235.

Synnefa, A., M. Santamouris, et al. (2007). "Estimating the effect of using cool coatings on energy loads and thermal comfort in residential buildings in various climatic conditions." Energy and Buildings **39**(11): 1167-1174.

Synnefa, A., M. Santamouris, et al. (2007). "On the development, optical properties and thermal performance of cool colored coatings for the urban environment." Solar Energy **81**(4): 488-497.

Taha, H. (1997). "Modeling the impacts of large-scale albedo changes on ozone air quality in the South Coast Air Basin." Atmospheric Environment **31**(11): 1667-1676.